lymphatics

MDPI

Article

Gata3 Insufficiency Accelerates Recanalization of Damaged Lymphatics via Adjusting Collagen Composition

Moyuru Hayashi [1], Takuya Harada [1], Jun Takai [2], Satoshi Uemura [2], Takashi Moriguchi [2], Tomomi Watanabe-Asaka [1,*] and Yoshiko Kawai [1,*]

[1] Division of Physiology, School of Medicine, Tohoku Medical and Pharmaceutical University, Sendai 983-8536, Japan; mhayashi@tohoku-mpu.ac.jp (M.H.); 22023013@is.tohoku-mpu.ac.jp (T.H.)
[2] Division of Medical Biochemistry, School of Medicine, Tohoku Medical and Pharmaceutical University, Sendai 983-8536, Japan; j-takai@tohoku-mpu.ac.jp (J.T.); s-uemura@tohoku-mpu.ac.jp (S.U.); moriguchi@tohoku-mpu.ac.jp (T.M.)
* Correspondence: twatana@tohoku-mpu.ac.jp (T.W.-A.); ykawai@tohoku-mpu.ac.jp (Y.K.); Tel.: +81-22-290-8716 (T.W.-A.); +81-22-290-8715 (Y.K.)

Abstract: The impaired repair of lymphatic vessels after tissue damage is an etiological hallmark of lymphedema. Previously, we demonstrated that lymphatic recanalization after the popliteal lymph node extirpation was delayed in *Gata2* heterozygous mice. This impaired lymphatic vessel recanalization in *Gata2* heterozygous mice was mitigated by administrating atelocollagen or crossing with heterozygous *Gata3* deletion mice. To clarify the potential involvement of *Gata3* heterozygosity in collagen gene expression within subdermal tissue, we conducted an RNAseq analysis and found 273 genes with up and 522 genes with down expression in *Gata3* heterozygous mice, and these genes were categorized as collagen and extracellular matrix-related genes by GO analysis. We also found that *Col6a1*, *a2*, and *a3*, which compose type VI collagen, underwent a transient but significant upregulation during the lymphatic recanalization process. Histological analysis revealed that the collagen structure in the subdermal tissue exhibited thinner collagen fiber in *Gata3* heterozygous deficient mice. These findings suggest that the altered collagen pattern in *Gata3* heterozygous mice contributed to the enhanced lymphatic vessel recanalization in *Gata2* heterozygous mice. The altered collagen expression pattern might play a role in shaping and maintaining the subcutaneous microenvironment.

Keywords: Gata3; connective tissue; type VI collagen

check for updates

Academic Editor: Noah Isakov

Received: 21 January 2025
Revised: 26 February 2025
Accepted: 4 March 2025
Published: 6 March 2025

Citation: Hayashi, M.; Harada, T.; Takai, J.; Uemura, S.; Moriguchi, T.; Watanabe-Asaka, T.; Kawai, Y. *Gata3* Insufficiency Accelerates Recanalization of Damaged Lymphatics via Adjusting Collagen Composition. *Lymphatics* **2025**, *3*, 7. https://doi.org/10.3390/lymphatics3010007

Copyright: © 2025 by the authors. Licensee MDPI, Basel, Switzerland. This article is an open access article distributed under the terms and conditions of the Creative Commons Attribution (CC BY) license (https://creativecommons.org/licenses/by/4.0/).

1. Introduction

Lymphatic vessels transport lymphatic fluid, which plays a central role in maintaining systemic homeostasis. Lymphatic fluid is vital for removing waste products and regulating interstitial fluid levels. Lymphedema, characterized by abnormally swollen extremities due to lymph accumulation, occurs when tissue damage or impaired lymphatic contraction disrupts smooth lymphatic flow. Lymphedema often appears secondary to cancer surgery, radiation therapy, or infectious diseases, whereas idiopathic/primary lymphedema sporadically occurs, albeit a smaller fraction [1,2]. It has been proposed that fibrosis is related to secondary lymphedema; nevertheless, the specific mechanism by which this occurs remains to be fully elucidated [3,4]. The prognosis for lymphedema patients tends to be unfavorable, and thus, breakthrough therapy or novel prevention strategies have long been awaited. The coordinated regeneration of functional lymphatic vessels upon surgical invasion or inflammatory insults holds the key for the prevention of secondary lymphedema.

GATA2 is a transcription factor with a zinc finger motif, the absence of which in the vascular system leads to systemic edema resulting in midgestational lethality in mice [5]. Additionally, heterozygous *Gata2* mutation is responsible for the occurrence of Emberger syndrome, which presents a form of hereditary lymphedema [6,7]. Our research has been focusing on the physiological function of lymphatic vessels, with a particular emphasis on the GATA transcription factor family. Our previous findings have demonstrated that the recanalization of lymphatic vessels after resecting lymph nodes was delayed in *Gata2* heterozygous deficient mice. This delay in lymphatic recanalization was not due to the decreased proliferation of lymphatic endothelial cells, suggesting that the surrounding microenvironment, including collagen accumulation, was important for lymphatic recanalization [8]. Additionally, the compound heterozygous knockout of *Gata2* and *Gata3* showed less severe lymphatic failure than in *Gata2* single heterozygous deficient mice. Additionally, we have demonstrated that the delayed lymphatic recanalization observed in *Gata2*$^{+/-}$ mice was also ameliorated by the addition of atelocollagen to the incision site [9]. Consequently, it seemed that collagen composition in subdermal tissue would be important to the microenvironment.

GATA3, a member of the GATA transcription factor family, plays a crucial role in lymph node development and T lymphocyte differentiation [10–12]. The elongation and remodeling of lymphatic vessels require an appropriate softness of the surrounding connective tissue [13,14]. Wound healing often involves the activity of endothelial cells and fibroblasts [15,16]. Since *Gata3*$^{+/-}$ ameliorates delayed recanalization in *Gata2*$^{+/-}$ mice, despite lacking its expression in lymphatic endothelial cells, we hypothesized the potential impact of *Gata3* heterozygosity on the microenvironment, especially in collagen composition. Meanwhile, the *Gata3* expression profile in subdermal fibroblasts and its potential role in lymphatic regeneration remain to be elucidated. To address these issues, we elucidated the expression profile of *Gata3* and asked whether the subcutaneous tissue structure was affected in *Gata3* heterozygous deficient mice. Moreover, we delved into the factors by which *Gata3* heterozygosity improves impaired lymphatic vessel recanalization in *Gata2* heterozygous deficient mice.

2. Results

2.1. Different Gene Expression Patterns in the Subcutaneous Tissue of the Popliteal Region of Gata3$^{+/-}$ *Mice*

To compare gene expression in the popliteal tissue of wild-type, *Gata2*$^{+/-}$, and *Gata3*$^{+/-}$ mice, two RNA samples from each of the remaining subcutaneous connective tissue genotypes were extracted after the removal of the popliteal lymph nodes and subjected to RNAseq analysis (Figure 1). Principal component analysis revealed that *Gata3*$^{+/-}$ and wild-type samples could be classified into a distinct group. However, *Gata2*$^{+/-}$ mice tissues, despite having the same genotype, exhibited considerable variability, rendering genotypic categorization challenging. (Figure 1A, right panel) Therefore, the following analyses were conducted to compare the wild-type and *Gata3*$^{+/-}$ mice.

By a comparison of gene expression in *Gata3*$^{+/-}$ and wild-type popliteal subcutaneous cells, conducted using the DESeq2 algorithm, a total of 795 genes were differentially expressed, of which 273 genes were upregulated and 522 genes were downregulated in *Gata3*$^{+/-}$ heterozygous cells (Figure 1B). Next, the 795 differentially expressed DEGs screened were analyzed by GO functional clustering and classified into molecular functions (Figure 1C). The prominent enriched terms of the upregulated differentially expressed genes in *Gata3*$^{+/-}$ mice were the cytoskeleton and collagen binding. The prominent enriched terms of the downregulated differentially expressed genes were ECM and cell–cell adhesion. In addition, the *Gata3* gene was downregulated in *Gata3* heterozygous tissue (Figures 1C and 2A).

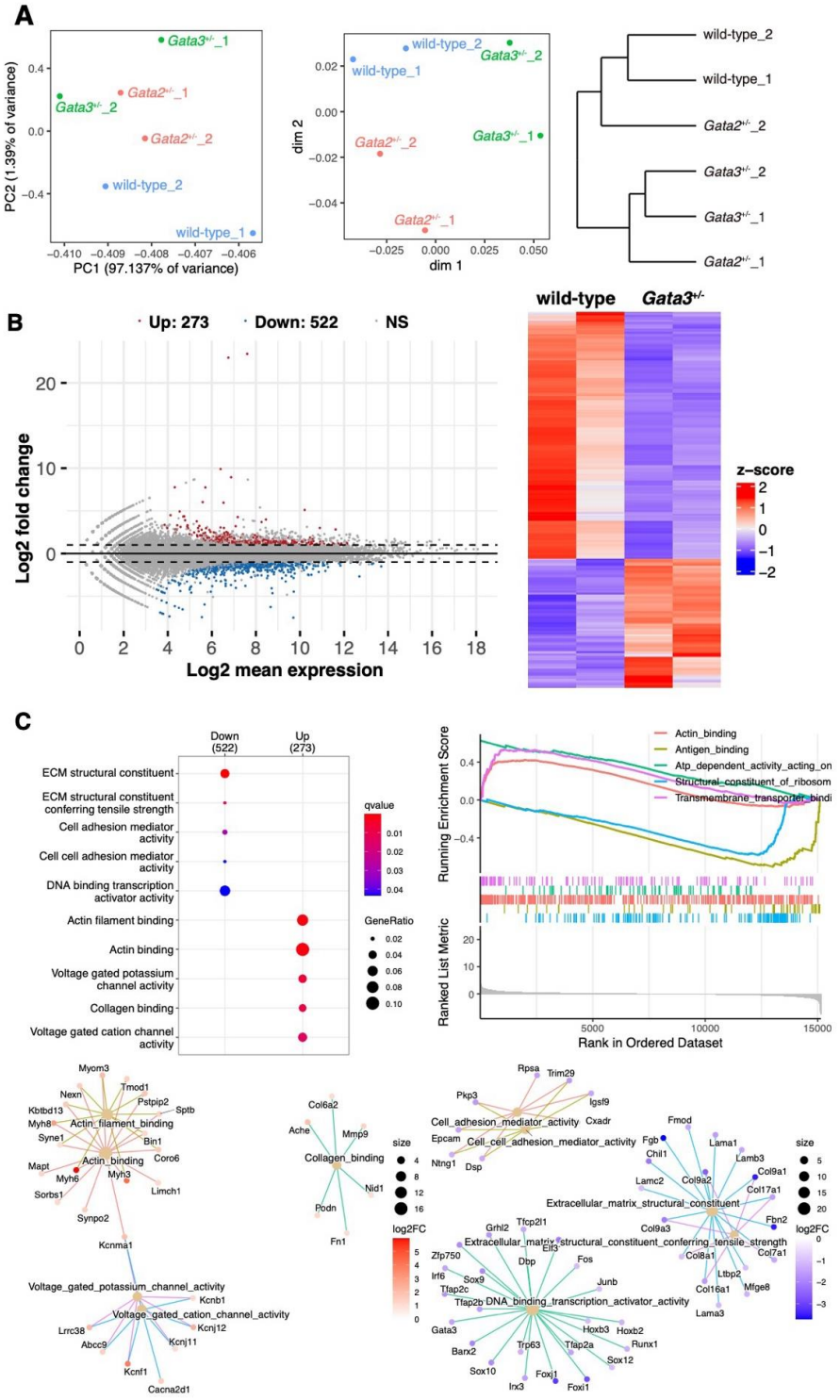

Figure 1. Transcriptome analyses of wild-type, *Gata2*$^{+/-}$, and *Gata3*$^{+/-}$ popliteal granule. (**A**) Principal component analysis, multi-dimensional scaling, and ward.D2 hierarchical clustering of two wild-type, two *Gata2*$^{+/-}$, and two *Gata3*$^{+/-}$ samples. (**B**) MA-plot and heatmap of DEG analysis between wild-type and *Gata3*$^{+/-}$ mice. In MA-plots, the log2-fold change indicates the mean expression level for each gene. Dashed lines indicate Log fold change = 1 or = −1. Each dot represents one gene. Gray dots represent no significant DEGs between wild-type and *Gata3*$^{+/-}$ mice, the blue dots represent downregulated genes, and red dots represent upregulated genes. (**C**) Over-representative analysis, GSEA (gene set enrichment analysis), gene-concept network (cnet) plot of DEGs between wild-type and *Gata3*$^{+/-}$ with GO functional clustering of molecular functions.

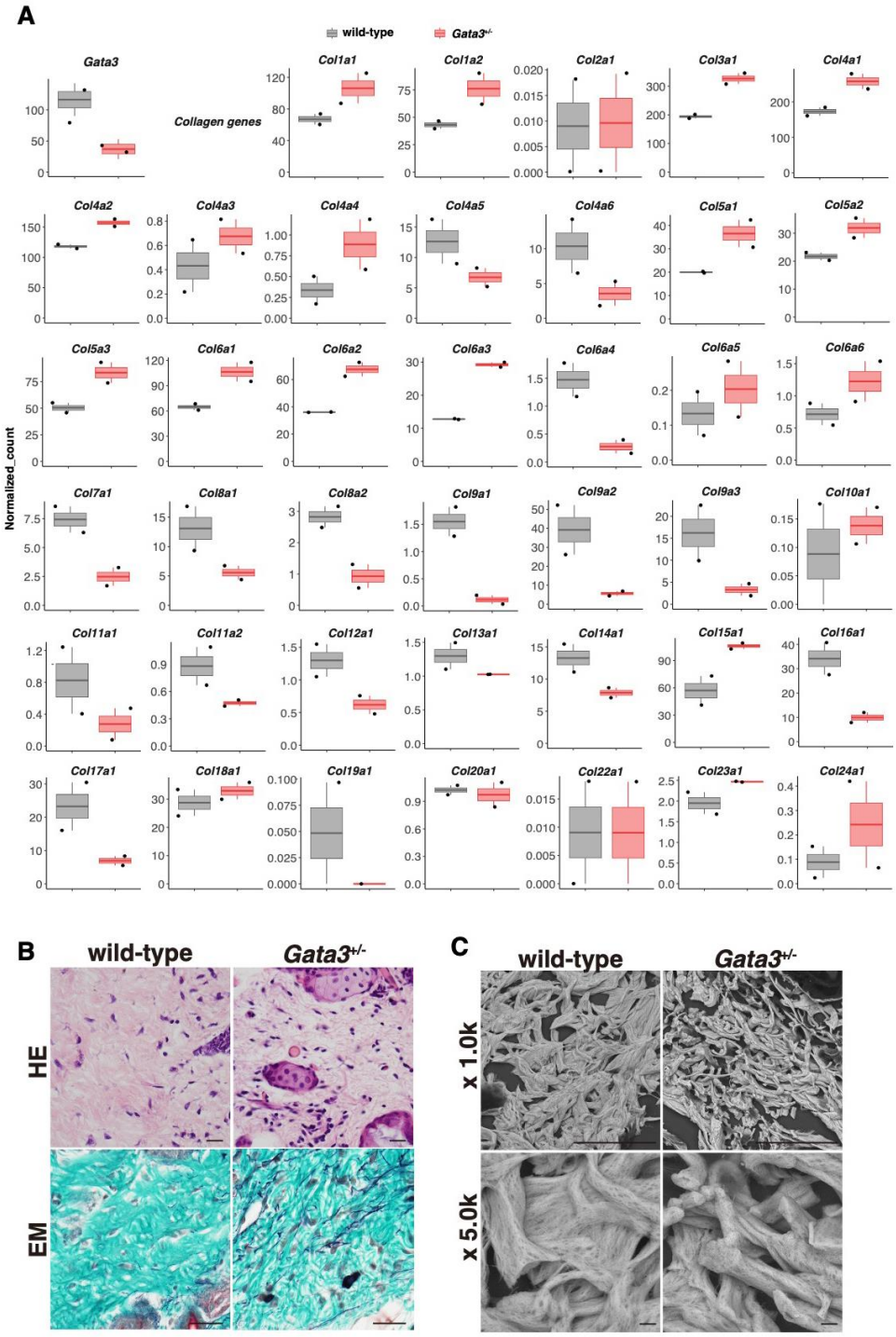

Figure 2. GOI profiling and histology of wild-type and *Gata3*$^{+/-}$ popliteal skin. (**A**) Box plot of *Gata3* and *collagen* genes. Gray and red bars indicate wild-type and *Gata3*$^{+/-}$ mice, respectively. (**B**,**C**) Representative images of the skin from the popliteal area in wild-type (left) and *Gata3*$^{+/-}$ (right) mice. (**B**) HE and Elastica-Masson (EM) staining. Scale bars are 20 μm. (**C**) Representative SEM images. Scale bars are 2 μm.

2.2. Altered Expression of the Collagen Gene Cluster and the Presence of Thin Dermal Collagen Fibers in Gata3$^{+/-}$ *Skin*

A comparative analysis of the expression of several collagen genes in the RNAseq dataset showed that specific collagen types exhibited characteristic up- or downregulation in the popliteal subcutaneous tissue of *Gata3*$^{+/-}$ mice (Figure 2A). The gene expression of *col7a1*, *col8a*, *col9a*, and *col16a1*, which are components of collagen type VII, VIII, IX, and

XVI, respectively, was reduced in *Gata3*$^{+/-}$ mice. On the other hand, the gene expression of *col1a*, *col3a*, and *col5a*, which are components of type I, II, III, and V collagens, the major subcutaneous fibril-forming collagens, was increased in *Gata3*$^{+/-}$. Type IX, XII, XIV, and XVI collagens, which are "fibril-associated collagens with interrupted triple helices (FACIT collagen)", and type VII collagen have an important function in collagen–collagen and cell interactions. The RNAseq results suggested that the shape of collagen fibers may be altered.

Accordingly, histological evaluations of the collagen fibers in the popliteal skin were conducted. After Elastica-Masson (EM) staining, which can detect collagen in green and elastic fibers in blue-black, the collagen fibers in the hypodermis of the popliteal region of *Gata3*$^{+/-}$ mice were observed to be thin and undulated (Figure 2B). Additionally, elastic fibers were prominent. Subsequently, scanning electron microscopy was employed to examine the structure of subcutaneous collagen fibers after periodic acid–methenamine–silver (PAM) staining. In *Gata3*$^{+/-}$ mice, collagen fibers exhibit a tendency to be less parallel in orientation and to have thinner fiber bundles (Figure 2C).

2.3. Transient Upregulation of Col6a Genes During Lymphatic Vessel Recanalization

The delay in the lymphatic recanalization was considerably improved with *Gata3* heterozygosity in *Gata2*$^{+/-}$ [8]. Therefore, we elucidated the gene expression during recanalization processes in *Gata3*$^{+/-}$ mice to determine whether it changes the gene expression. In this study, the expression levels of *Col6a1*, *6a2*, and *6a3*, which were found to be elevated in subcutaneous *Gata3*$^{+/-}$ mice under stable conditions, were subjected to qPCR-based evaluation prior to and following surgical intervention. In the wild type, the three *Col6a* genes exhibited transient upregulation in the ratio of their expression to that of *β-actin*, peaking at one week after surgery (Figure 3). These results suggested that there were substantial alterations in collagen gene expressions in fibroblasts approximately one week into the lymphatic recanalization processes. In contrast, in *Gata3*$^{+/-}$ mice, *Col6a1* and *6a3* exhibited analogous alterations in the wild type and *Col6a2* expression remained unaltered, irrespective of the occurrence of lymphatic vessel recanalization. These findings suggested that disparities in gene expression were evident not only in steady-state conditions but also during the process of lymphatic vessel recanalization in *Gata3*$^{+/-}$ mice.

3. Discussion

In the present study, we hypothesized that the improvement in delayed lymphatic recanalization in *Gata2*$^{+/-}$::*Gata3*$^{+/-}$ mice is due to changes in the microenvironment surrounding the lymphatic vessels in *Gata3*$^{+/-}$ mice. To elucidate our hypothesis, we conducted analyses of the popliteal subcutaneous gene expression and histology of *Gata3*$^{+/-}$ mice, and revealed the distinct gene expression of various collagens and altered collagen fibers in *Gata3*$^{+/-}$ mice compared to the wild type.

In *Gata3*$^{+/-}$ heterozygous mice, RNAseq analysis demonstrated a reduction in the expression levels of *Col9a1*, *2*, and *3* genes, which constitute type IX collagen. Type IX collagen is a member of the FACIT-type collagen, which is involved in the assembly of collagen fibrils with other extracellular matrix (ECM) components through interactions with the surrounding environment of other collagen fibrils [17–21]. While fibrillar collagens and network-forming collagens are the main components of the collagenous ECM, FACITs are thought to play a delicate and unique role by forming molecular bridges, thereby facilitating the stability of the collagenous network in the ECM [21]. In this study, the expression of *Col7a1*, a component of type VII collagen, which is an anchoring fibril protein, was also markedly decreased. The result that the interaction between collagen fibers was diminished in *Gata3*$^{+/-}$ mice suggested the subcutaneous accumulation of attenuated collagen fibers. In fact, the skin of Gata3 heterozygous mice exhibits hyperextensible

traits in comparison to wild-type mice. This phenomenon is expected to be related with alterations in collagen-related gene expression.

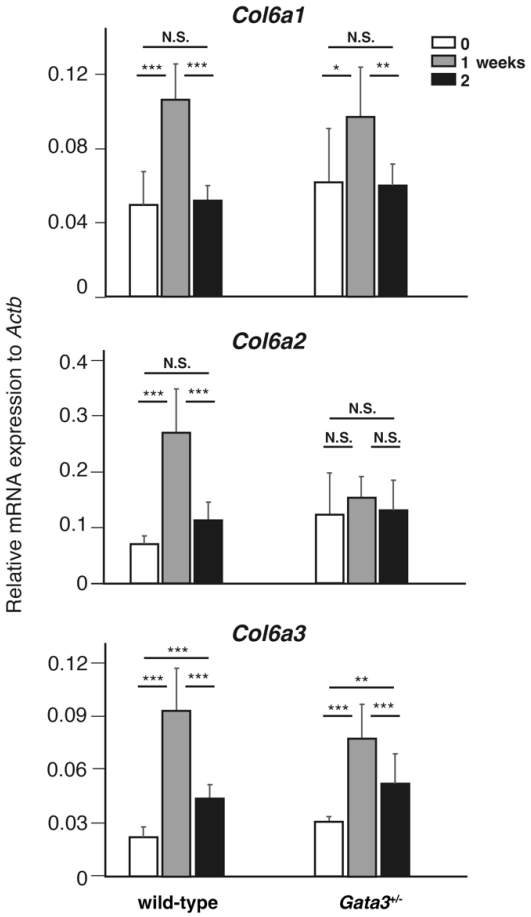

Figure 3. Expression patterns of *col6a* genes after lymph node extirpation in wild-type and *Gata3*$^{+/-}$ mice. The mRNA expression of *Col6a1*, *2*, and *3* in the popliteal granulation of wild-type and *Gata3*$^{+/-}$ mice. The relative mRNA levels were based on the β-*actin*. The white-, gray-, and black-colored columns indicate 0, 1, and 2 weeks after the popliteal lymph node extirpation, respectively. Eight samples were analyzed in each condition. Error bars indicate S.D. * $p < 0.05$; ** $p < 0.01$; *** $p < 0.005$; N.S. not significant.

The presence of the distinct shape of collagen fibers in the dermis of *Gata3*$^{+/-}$ mice in the histological analysis suggested that the subcutaneous structure under normal conditions differed from that of the wild type. In this study, we found that *Col6a1*, *a2*, and *a3*, which constitute type VI collagen, were slightly upregulated in *Gata3*$^{+/-}$ mice under normal conditions. Furthermore, qPCR results demonstrated that *Col6a* genes were upregulated one week after lymph node excision. The increase in *Col6a2* expression one week after lymph node extirpation was suppressed in *Gata3*$^{+/-}$ mice. These results suggest that, in addition to the effects on subcutaneous tissue structure due to the altered homeostatic expression of *Col6a* genes under normal conditions, differences in these gene expression after surgery may also affect lymphatic recanalization. Type VI collagen is a molecule that forms heterotrimers of Col6a1, a2, and a3 chains and is recognized extracellularly as a bead-like or microfibril structure that functions to bind the basement membrane and collagen fibers. The association of the basement membrane with fibrillar-type collagen is expected to significantly alter the subcutaneous structure. The association of the basement membrane with fibrillar-type collagen is expected to result in substantial alterations to the subcutaneous structure including the hardness–softness. Proper softness of the surrounding

tissue is crucial for the development or regeneration of lymphatic vessels [14]. The results in this study demonstrated that a heterozygous deletion of *Gata3* affects the shape of collagen fibers, which can be explained consistently with the aforementioned findings in which the delayed lymphatic recanalization observed in *Gata2*$^{+/-}$ mice was ameliorated by the addition of atelocollagen [9].

Collagen is a protein that is abundantly expressed in the skin. Abnormalities in collagen can result in various diseases that specifically affect connective tissue [22–25]. For instance, Ehlers–Danlos syndrome (Collagen1,3,5,12) [26,27], Stickler syndrome (collagen9a, 11) [28–30], and epidermolysis bullosa (collagen7) [31,32] are prominent diseases characterized by abnormal subcutaneous connective tissues. However, all of these conditions are intractable and challenging to treat. Given the finding that *Gata3* heterozygous knockout mice are deaf [33], *Gata3*$^{+/-}$ mice may serve as suitable models for further investigation into diseases with connective tissue. The relationship between these diseases and lymphatic vessels is a subject for future studies.

Regarding lymphedema and fibrosis, in our murine experiments, we observed lymphatic recanalization in the acute phase following lymph node excision, thereby precluding confirmation of the symptoms associated with lymphedema. Fibroblast function is crucial for immunity and for fibrosis in the skin [34–36]. The analysis of the severity of human lymphedema and its treatment are reported, including in papers by Hayashida et al. [37]. Moreover, recent findings have emerged regarding the relationship between secondary lymphedema and fibrosis [38,39]. Gata3, which is expressed in Th2, can also be related to immunity and fibrosis. In the future, we aim to examine the scarring after lymph node excision and the efficacy of collagen treatment for therapeutic application to patients with secondary lymphedema.

4. Materials and Methods

4.1. Mice

Gata3 LacZ knock-in (*Gata3*$^{+/-}$) mice carry LacZ reporter genes that are inserted into the translational initiation site of *Gata3* alleles [40,41]. The primers used for genotyping are listed in Table 1. Experiments were performed using 6-to-8-week-old mice. All surgeries were performed under a combination anesthetic (medetomidine/midazolam/utorphanol: 0.3/4/5) prepared with 0.3 mg/kg Medetomidine Hydrochloride, 4.0 mg/kg Midazolam, and 5.0 mg/kg Butorphanol Tartrate by intraperitoneal injection [42], and all efforts were made to minimize suffering.

Table 1. Sequences of primers.

Gene	Sense Primer	Antisense Primer	Assay
Gata3^{LacZ}	TTCGCCAGCTGGCGTAATAGCGAAGAGGC	TAGGTCACGTTGGTGTAGATGGGCGCATCG	genotyping
Col6a1	AACAGGAATAGGAAATGTGACCC	ACACCACGGATAGGTTAGGGG	qPCR
Col6a2	AAGGCCCCATTGGATTCCC	CTCCCTTCCGACCATCCGAT	qPCR
Col6a3	GCTGCGGAATCACTTTGTGC	CACCTTGACACCTTTCTGGGT	qPCR
β-actin	AGATCAAGATCATTGCTCCTCCT	ACGCAGCTCAGTAACAGTCC	qPCR

4.2. Popliteal Lymph Node Extirpation

The procedure for the lymph node extirpation and evaluation of lymphatic recanalization was referred in Watanabe-Asaka et al. [8]. In brief, 0.1% Evans Blue (EB) dye was injected into the mouse footpad subdermal space to visualize the popliteal lymph node. After the footpad massage, the popliteal lymph nodes on both sides were excised. For RNAseq, subcutaneous tissue surrounding the excised lymph nodes was sampled immediately after the lymph node excision in an effort to avoid the inclusion of muscle tissues.

For qPCR analysis, the skin incision was closed with surgical sutures (No.21 Mani inc., Utsunomiya, Japan) for later analysis.

4.3. RNA-Seq and Bioinformatic Analysis

Dermal tissues were obtained from both sides after popliteal node excision, and 3 *Gata3*$^{+/-}$ and 3 wild-type mice were collected. Total RNA was isolated using RNeasy® Micro kit (QIAGEN, Hilden, Germany) according to the manufacturer's instructions and eluted in a final volume of 25 µL. RNA quality was assessed using a 4200 TapeStation System (Agilent Technologies, Santa Clara, CA, USA). RNA samples were submitted to Rhelixa, Inc. (Tokyo, Japan) and sequenced using eukaryote RNA-seq standard basic plan. Poly-A selected total RNA for *Gata3*$^{+/-}$ and wild-type samples were sequenced using Illumina NovaSeq 6000 platform using the strand-specific, paired-end module with a read length of 150 bp (n = 2 each). Raw data were quality-checked using the FastQC program (Version 0.11.7; https://www.bioinformatics.babraham.ac.uk/projects/fastqc/ (accessed on 7 May 2024)) [43]. Low-quality (<20) bases and adapter sequences were trimmed by Trimmomatic software (Version 0.38) [44] with the following parameters: ILLUMINACLIP: path/to/adapter.fa:2:30:10 LEADING:20 TRAILING:20 SLIDINGWINDOW:4:15 MINLEN:36. The trimmed reads were aligned to the reference genome (mm10) using RNA-seq aligner HISAT2 [45] (Version 2.1.0) and results were converted into .bam files with Samtools [46] (Version 1.9). The .bam files were used to estimate the abundance of uniquely mapped reads with featureCounts [47] (Version 1.6.3) for the following analysis. The raw datasets used during our study are available through DDBJ Database Accession number PRJDB19946.

For the bioinformatic analysis, DESeq2 [48] in the RNAseqChef platform [49] (v1.1.3) was used to analyze the differential expression of mRNAs between *Gata3*$^{+/-}$ and wild-type groups. Those transcripts with the parameters of an absolute fold change (FC) of $\geq$2 and a false discovery rate (FDR) of <0.05 were considered to be differentially expressed. The enrichment analysis of Gene Ontology (GO) was performed based on molecular functions (http://www.geneontology.org/ (accessed on 9 September 2024)) by choosing the differentially expressed coding RNAs. All above analysis results meeting the condition of $p < 0.05$ were considered to be significant.

4.4. Histology

The dermis was fixed with skin overnight in 4% paraformaldehyde in PBS at 4 °C and then processed for staining as paraffin-embedded sections (4 µm). The sections were stained with HE. Elastica-Masson (EM) staining was performed to evaluate collagen and elastic fibers [50,51].

Images were visualized using a Nikon ECLIPSE Ni-U upright microscope (Tokyo, Japan). Images were captured using a Nikon DS-Fi3 camera and the NIS-Elements software (v5.11).

4.5. Scanning Electron Microscopy (SEM)

For SEM, 4 µm thickness paraffin embedded sections were rehydrated, and we performed periodic acid–methenamine–silver (PAM) staining following the standard protocol. SEM images were collected using a Miniscope TM4000 (Hitachi High-Technologies, Co., Hitachi, Japan) scanning electron microscope operated at 15.0 kV. Images were acquired at 1000 and 5000× direct magnifications.

4.6. cDNA Synthesis and RT-PCR Analysis

The mRNA expression of genes related to lymphangiogenesis was evaluated by quantitative RT-PCR (qRT-PCR). Total RNA was extracted from the granulation tissues around the popliteal lymph vessels using TRIzol™ reagent (Thermo Fisher Scientific, Tokyo, Japan) 0, 1,

or 2 weeks after the surgery. The extracted RNA was subjected to reverse transcription with a High-Capacity cDNA Reverse Transcription Kit (Thermo Fisher Scientific). Next, 1.0 μg of total RNA was used to synthesize the cDNA. The primers used for genotyping and qRT-PCR are listed in Table 1. cDNA was diluted twenty-fold before PCR amplification. qRT-PCR was performed using a QuantStudio 3 (Thermo Fisher Scientific). Negative controls were included in each reaction, and PCR products obtained with each primer pair were subjected to analysis by the ΔCt method. *Actb* was used as an internal reference. The data were analyzed with QuantStudio Design & analysis Software v1.2.

4.7. Statistical Analysis

Means and standard deviations were calculated. Data were subjected to one-way analysis of variance using Microsoft Excel software (Microsoft Co., Redmond, WA, USA) at a significance level of 0.05. Analyses were performed using Student's *t* test and chi-square test, as appropriate.

Author Contributions: Conceptualization, M.H., T.W.-A. and Y.K.; data curation, M.H., T.H., T.W.-A. and Y.K.; formal analysis, M.H., T.H., J.T., S.U. and T.W.-A.; investigation, M.H., T.H., T.W.-A. and Y.K.; methodology, J.T., S.U., T.W.-A. and Y.K.; resource, J.T., S.U. and T.M.; writing—original draft preparation, T.W.-A. writing—review and editing, M.H., T.M., T.W.-A. and Y.K.; visualization, M.H., T.H. and T.W.-A.; supervision, T.M. and Y.K.; project administration, T.W.-A. and Y.K.; funding acquisition, T.W.-A. All authors have read and agreed to the published version of the manuscript.

Funding: This research was funded by the Grants-in-Aid for Scientific Research (JSPS Kakenhi Grant Number JP23K07165 to TW-A) from the Ministry of Education, Culture, Sports, Science, and Technology (MEXT) of Japan.

Institutional Review Board Statement: The animal study protocol was approved by the Committee on the Ethics of Animal Experiments of Tohoku Medical and Pharmaceutical University (Permit Number: 21002-cn, 22004-cn, 23011-cn, and 24011-cn) in accordance with ARRIVE guidelines (https://arriveguidelines.org (accessed on 22 March 2024)) and the Japanese laws and guidelines for the care of experimental animals according to the Animal Experiment Enforcement Rule of Tohoku Medical and Pharmaceutical University.

Informed Consent Statement: Not applicable.

Data Availability Statement: Raw data supporting these conclusions will be available on request to the authors.

Acknowledgments: We express our appreciation to Waka Yamashita, Ayano Miura, and Chihiro Oto for helping with the data collection. We are grateful to the Center of Laboratory Animal Science, Fukumuro branch, for helping with animal care and the Histopathology Core Facility for supporting histological experiments.

Conflicts of Interest: The authors declare no conflicts of interest.

References

1. Grada, A.A.; Phillips, T.J. Lymphedema: Pathophysiology and clinical manifestations. *J. Am. Acad. Dermatol.* **2017**, *77*, 1009–1020. [CrossRef] [PubMed]
2. Rockson, S.G. Advances in Lymphedema. *Circ. Res.* **2021**, *128*, 2003–2016. [CrossRef] [PubMed]
3. Kataru, R.P.; Wiser, I.; Baik, J.E.; Park, H.J.; Rehal, S.; Shin, J.Y.; Mehrara, B.J. Fibrosis and secondary lymphedema: Chicken or egg? *Transl. Res.* **2019**, *209*, 68–76. [CrossRef]
4. Brown, S.; Dayan, J.H.; Kataru, R.P.; Mehrara, B.J. The Vicious Circle of Stasis, Inflammation, and Fibrosis in Lymphedema. *Plast. Reconstr. Surg.* **2023**, *151*, 330e–341e. [CrossRef] [PubMed]
5. Kazenwadel, J.; Betterman, K.L.; Chong, C.E.; Stokes, P.H.; Lee, Y.K.; Secker, G.A.; Agalarov, Y.; Demir, C.S.; Lawrence, D.M.; Sutton, D.L.; et al. GATA2 is required for lymphatic vessel valve development and maintenance. *J. Clin. Investig.* **2015**, *125*, 2979–2994. [CrossRef] [PubMed] [PubMed Central]

6. Ostergaard, P.; Simpson, M.A.; Connell, F.C.; Steward, C.G.; Brice, G.; Woollard, W.J.; Dafou, D.; Kilo, T.; Smithson, S.; Lunt, P.; et al. Mutations in GATA2 cause primary lymphedema associated with a predisposition to acute myeloid leukemia (Emberger syndrome). *Nat. Genet.* **2011**, *43*, 929–931. [CrossRef] [PubMed]
7. Polat, A.; Dinulescu, M.; Fraitag, S.; Nimubona, S.; Toutain, F.; Jouneau, S.; Poullot, E.; Droitcourt, C.; Dupuy, A. Skin manifestations among GATA2-deficient patients. *Br. J. Dermatol.* **2018**, *178*, 781–785. [CrossRef] [PubMed]
8. Watanabe-Asaka, T.; Hayashi, M.; Uemura, S.; Takai, J.; Suzuki, A.; Moriguchi, T.; Kawai, Y. GATA2 participates in the recanalization of lymphatic vessels after surgical lymph node extirpation. *Genes Cells* **2021**, *26*, 474–484. [CrossRef] [PubMed]
9. Watanabe-Asaka, T.; Hayashi, M.; Harada, T.; Uemura, S.; Takai, J.; Nakamura, Y.; Moriguchi, T.; Kawai, Y. Perturbed collagen metabolism underlies lymphatic recanalization failure in Gata2 heterozygous deficient mice. *J. Biochem.* **2024**, *175*, 551–560. [CrossRef] [PubMed]
10. Ho, I.C.; Tai, T.S.; Pai, S.Y. GATA3 and the T-cell lineage: Essential functions before and after T-helper-2-cell differentiation. *Nat. Rev. Immunol.* **2009**, *9*, 125–135. [CrossRef] [PubMed] [PubMed Central]
11. Yagi, R.; Zhu, J.; Paul, W.E. An updated view on transcription factor GATA3-mediated regulation of Th1 and Th2 cell differentiation. *Int. Immunol.* **2011**, *23*, 415–420. [CrossRef] [PubMed] [PubMed Central]
12. Bovay, E.; Sabine, A.; Prat-Luri, B.; Kim, S.; Son, K.; Willrodt, A.H.; Olsson, C.; Halin, C.; Kiefer, F.; Betsholtz, C.; et al. Multiple roles of lymphatic vessels in peripheral lymph node development. *J. Exp. Med.* **2018**, *215*, 2760–2777. [CrossRef] [PubMed] [PubMed Central]
13. Yang, Y.; Oliver, G. Development of the mammalian lymphatic vasculature. *J. Clin. Investig.* **2014**, *124*, 888–897. [CrossRef] [PubMed] [PubMed Central]
14. Frye, M.; Taddei, A.; Dierkes, C.; Martinez-Corral, I.; Fielden, M.; Ortsäter, H.; Kazenwadel, J.; Calado, D.P.; Ostergaard, P.; Salminen, M.; et al. Matrix stiffness controls lymphatic vessel formation through regulation of a GATA2-dependent transcriptional program. *Nat. Commun.* **2018**, *9*, 1511. [CrossRef] [PubMed] [PubMed Central]
15. Ross, R. The fibroblast and wound repair. *Biol. Rev. Camb. Philos. Soc.* **1968**, *43*, 51–96. [CrossRef] [PubMed]
16. Knoedler, S.; Broichhausen, S.; Guo, R.; Dai, R.; Knoedler, L.; Kauke-Navarro, M.; Diatta, F.; Pomahac, B.; Machens, H.G.; Jiang, D.; et al. Fibroblasts—The cellular choreographers of wound healing. *Front. Immunol.* **2023**, *14*, 1233800. [CrossRef] [PubMed] [PubMed Central]
17. van der Rest, M.; Mayne, R.; Ninomiya, Y.; Seidah, N.G.; Chretien, M.; Olsen, B.R. The structure of type IX collagen. *J. Biol. Chem.* **1985**, *260*, 220–225. [CrossRef] [PubMed]
18. van der Rest, M.; Dublet, B.; Champliaud, M.F. Fibril-associated collagens. *Biomaterials* **1990**, *11*, 28–31. [PubMed]
19. Sun, B. The mechanics of fibrillar collagen extracellular matrix. *Cell Rep. Phys. Sci.* **2021**, *2*, 100515. [CrossRef] [PubMed] [PubMed Central]
20. He, Y.; Sardar, S.; Bay-Jensen, A.C.; Port, H.; Karsdal, M.A. Chapter 9—Type IX collagen. In *Biochemistry of Collagens, Laminins and Elastin*, 3rd ed.; Karsdal, M.A., Ed.; Academic Press: Cambridge, MA, USA, 2023; pp. 89–95. ISBN 9780443156175. [CrossRef]
21. Port, H.; He, Y.; Karsdal, M.A.; Madsen, E.A.; Bay-Jensen, A.C.; Willumsen, N.; Holm Nielsen, S. Type IX Collagen Turnover Is Altered in Patients with Solid Tumors. *Cancers* **2024**, *16*, 2035. [CrossRef]
22. Myllyharju, J.; Kivirikko, K.I. Collagens and collagen-related diseases. *Ann. Med.* **2001**, *33*, 7–21. [CrossRef] [PubMed]
23. Arseni, L.; Lombardi, A.; Orioli, D. From Structure to Phenotype: Impact of Collagen Alterations on Human Health. *Int. J. Mol. Sci.* **2018**, *19*, 1407. [CrossRef] [PubMed] [PubMed Central]
24. Nielsen, S.H.; Sardar, S.; Karsdal, M.A.; Henriksen, K. Chapter 36—Collagen diseases. In *Biochemistry of Collagens, Laminins and Elastin*, 3rd ed.; Karsdal, M.A., Ed.; Academic Press: Cambridge, MA, USA, 2023; pp. 371–398. ISBN 9780443156175. [CrossRef]
25. Salles Rosa Neto, N.; Pereira, I.A.; Sztajnbok, F.R.; Azevedo, V.F. Unraveling the genetic collagen connection: Clinical and therapeutic insights on genetic connective tissue disorders. *Adv. Rheumatol.* **2024**, *64*, 32. [CrossRef] [PubMed]
26. Malfait, F.; Francomano, C.; Byers, P.; Belmont, J.; Berglund, B.; Black, J.; Bloom, L.; Bowen, J.M.; Brady, A.F.; Burrows, N.P.; et al. The 2017 international classification of the Ehlers-Danlos syndromes. *Am. J. Med. Genet. C Semin. Med. Genet.* **2017**, *175*, 8–26. [CrossRef] [PubMed]
27. Malfait, F.; Castori, M.; Francomano, C.A.; Giunta, C.; Kosho, T.; Byers, P.H. The Ehlers-Danlos syndromes. *Nat. Rev. Dis. Primers* **2020**, *6*, 64. [CrossRef] [PubMed]
28. Nixon, T.R.W.; Alexander, P.; Richards, A.; McNinch, A.; Bearcroft, P.W.P.; Cobben, J.; Snead, M.P. Homozygous Type IX collagen variants (COL9A1, COL9A2, and COL9A3) causing recessive Stickler syndrome-Expanding the phenotype. *Am. J. Med. Genet. A* **2019**, *179*, 1498–1506. [CrossRef] [PubMed]
29. Nixon, T.R.W.; Richards, A.J.; Martin, H.; Alexander, P.; Snead, M.P. Autosomal Recessive Stickler Syndrome. *Genes* **2022**, *13*, 1135. [CrossRef] [PubMed] [PubMed Central]
30. Acke, F.R.E.; De Leenheer, E.M.R. Hearing Loss in Stickler Syndrome: An Update. *Genes* **2022**, *13*, 1571. [CrossRef]
31. Bardhan, A.; Bruckner-Tuderman, L.; Chapple, I.L.C.; Fine, J.D.; Harper, N.; Has, C.; Magin, T.M.; Marinkovich, M.P.; Marshall, J.F.; McGrath, J.A.; et al. Epidermolysis bullosa. *Nat. Rev. Dis. Primers* **2020**, *6*, 78. [CrossRef] [PubMed]
32. South, A.P.; Laimer, M.; Gueye, M.; Sui, J.Y.; Eichenfield, L.F.; Mellerio, J.E.; Nyström, A. Type VII Collagen Deficiency in the Oncogenesis of Cutaneous Squamous Cell Carcinoma in Dystrophic Epidermolysis Bullosa. *J. Investig. Dermatol.* **2023**, *143*, 2108–2119. [CrossRef] [PubMed]

33. van der Wees, J.; van Looij, M.A.; de Ruiter, M.M.; Elias, H.; van der Burg, H.; Liem, S.S.; Kurek, D.; Engel, J.D.; Karis, A.; van Zanten, B.G.; et al. Hearing loss following Gata3 haploinsufficiency is caused by cochlear disorder. *Neurobiol. Dis.* **2004**, *16*, 169–178. [CrossRef] [PubMed]
34. Baik, J.E.; Park, H.J.; Kataru, R.P.; Savetsky, I.L.; Ly, C.L.; Shin, J.; Encarnacion, E.M.; Cavali, M.R.; Klang, M.G.; Riedel, E.; et al. TGF-β1 mediates pathologic changes of secondary lymphedema by promoting fibrosis and inflammation. *Clin. Transl. Med.* **2022**, *12*, e758. [CrossRef] [PubMed]
35. Sano, M.; Hirakawa, S.; Sasaki, T.; Inuzuka, K.; Katahashi, K.; Kayama, T.; Yamanaka, Y.; Tsuyuki, H.; Endo, Y.; Naruse, E.; et al. Role of Subcutaneous Adipose Tissues in the Pathophysiology of Secondary Lymphedema. *Lymphat. Res. Biol.* **2022**, *20*, 593–599. [CrossRef]
36. Duhon, B.H.; Phan, T.T.; Taylor, S.L.; Crescenzi, R.L.; Rutkowski, J.M. Current Mechanistic Understandings of Lymphedema and Lipedema: Tales of Fluid, Fat, and Fibrosis. *Int. J. Mol. Sci.* **2022**, *23*, 6621. [CrossRef] [PubMed]
37. Hayashida, K.; Yoshida, S.; Yoshimoto, H.; Fujioka, M.; Saijo, H.; Migita, K.; Kumaya, M.; Akita, S. Adipose-Derived Stem Cells and Vascularized Lymph Node Transfers Successfully Treat Mouse Hindlimb Secondary Lymphedema by Early Reconnection of the Lymphatic System and Lymphangiogenesis. *Plast. Reconstr. Surg.* **2017**, *139*, 639–651. [CrossRef]
38. Will, P.A.; Kilian, K.; Bieback, K.; Fricke, F.; Berner, J.E.; Kneser, U.; Hirche, C. Lymphedema-Associated Fibroblasts Are Related to Fibrosis and Stage Progression in Patients and a Murine Microsurgical Model. *Plast. Reconstr. Surg.* **2024**, *154*, 688e–700e. [CrossRef]
39. Son, H.; Lee, S.; Kim, K.; Koo, K.I.; Hwang, C.H. Deep learning-based quantitative estimation of lymphedema-induced fibrosis using three-dimensional computed tomography images. *Sci. Rep.* **2022**, *12*, 15371. [CrossRef] [PubMed]
40. Pandolfi, P.P.; Roth, M.E.; Karis, A.; Leonard, M.W.; Dzierzak, E.; Grosveld, F.G.; Engel, J.D.; Lindenbaum, M.H. Targeted disruption of the GATA3 gene causes severe abnormalities in the nervous system and in fetal liver haematopoiesis. *Nat. Genet.* **1995**, *11*, 40–44. [CrossRef] [PubMed]
41. Moriguchi, T.; Takako, N.; Hamada, M.; Maeda, A.; Fujioka, Y.; Kuroha, T.; Huber, R.E.; Hasegawa, S.L.; Rao, A.; Yamamoto, M.; et al. Gata3 participates in a complex transcriptional feedback network to regulate sympathoadrenal differentiation. *Development* **2006**, *133*, 3871–3881. [CrossRef] [PubMed]
42. Kawai, S.; Takagi, Y.; Kaneko, S.; Kurosawa, T. Effect of three types of mixed anesthetic agents alternate to ketamine in mice. *Exp. Anim.* **2011**, *60*, 481–487. [CrossRef] [PubMed]
43. Cock, P.J.; Fields, C.J.; Goto, N.; Heuer, M.L.; Rice, P.M. The Sanger FASTQ file format for sequences with quality scores, and the Solexa/Illumina FASTQ variants. *Nucleic Acids Res.* **2010**, *38*, 1767–1771. [CrossRef] [PubMed] [PubMed Central]
44. Bolger, A.M.; Lohse, M.; Usadel, B. Trimmomatic: A flexible trimmer for Illumina sequence data. *Bioinformatics* **2014**, *30*, 2114–2120. [CrossRef] [PubMed] [PubMed Central]
45. Kim, D.; Langmead, B.; Salzberg, S.L. HISAT: A fast spliced aligner with low memory requirements. *Nat. Methods* **2015**, *12*, 357–360. [CrossRef] [PubMed] [PubMed Central]
46. Li, H.; Handsaker, B.; Wysoker, A.; Fennell, T.; Ruan, J.; Homer, N.; Marth, G.; Abecasis, G.; Durbin, R.; 1000 Genome Project Data Processing Subgroup. The Sequence Alignment/Map format and SAMtools. *Bioinformatics* **2009**, *25*, 2078–2079. [CrossRef] [PubMed] [PubMed Central]
47. Liao, Y.; Smyth, G.K.; Shi, W. featureCounts: An efficient general purpose program for assigning sequence reads to genomic features. *Bioinformatics* **2014**, *30*, 923–930. [CrossRef] [PubMed]
48. Love, M.I.; Huber, W.; Anders, S. Moderated estimation of fold change and dispersion for RNA-seq data with DESeq2. *Genome Biol.* **2014**, *15*, 550. [CrossRef] [PubMed] [PubMed Central]
49. Etoh, K.; Nakao, M. A web-based integrative transcriptome analysis, RNAseqChef, uncovers the cell/tissue type-dependent action of sulforaphane. *J. Biol. Chem.* **2023**, *299*, 104810. [CrossRef] [PubMed] [PubMed Central]
50. Yabe, Y.; Hagiwara, Y.; Ando, A.; Tsuchiya, M.; Minowa, T.; Takemura, T.; Honda, M.; Hatori, K.; Sonofuchi, K.; Kanazawa, K.; et al. Chondrogenic and fibrotic process in the ligamentum flavum of patients with lumbar spinal canal stenosis. *Spine* **2015**, *40*, 429–435. [CrossRef] [PubMed]
51. Yabe, Y.; Hagiwara, Y.; Tsuchiya, M.; Honda, M.; Hatori, K.; Sonofuchi, K.; Kanazawa, K.; Koide, M.; Sekiguchi, T.; Itaya, N.; et al. Decreased elastic fibers and increased proteoglycans in the ligamentum flavum of patients with lumbar spinal canal stenosis. *J. Orthop. Res.* **2016**, *34*, 1241–1247. [CrossRef] [PubMed]

Disclaimer/Publisher's Note: The statements, opinions and data contained in all publications are solely those of the individual author(s) and contributor(s) and not of MDPI and/or the editor(s). MDPI and/or the editor(s) disclaim responsibility for any injury to people or property resulting from any ideas, methods, instructions or products referred to in the content.